Journal for ImmunoTherapy of Cancer

Clinical outcomes and spatial transcriptomic profiles of CD19/20 CAR-T therapy in relapsed or refractory B-cell non-Hodgkin's lymphoma

Lixin Wang,[1] Chuling Fang ,[1] Yuanyuan Zheng,[1] Yuanyuan Xu,[1] Wenfa Huang,[1] Weiqiang Zhao,[1] Yiran Wang,[1] Jianglong Xia,[1] Kun Tan,[1] Lei Wang,[1] Huixin Peng,[1] Xiao Guo,[1] Shuhong Wang,[1] Lijun Wang,[1] Lian Liu,[1] Jingqiao Qiao,[1] Xiangyu Meng,[1] Ziqian He,[1] Zonghua Wen,[2] Chuan Yu,[3] Junhui Mei,[1] Hongxin Wang,[1] Yisheng Li,[3] Li Yu[1]

To cite: Wang L, Fang C, Zheng Y, *et al*. Clinical outcomes and spatial transcriptomic profiles of CD19/20 CAR-T therapy in relapsed or refractory B-cell non-Hodgkin's lymphoma. *Journal for ImmunoTherapy of Cancer* 2026;**14**:e015114. doi:10.1136/jitc-2026-015114

► Additional supplemental material is published online only. To view, please visit the journal online (https://doi.org/10.1136/jitc-2026-015114).

LW and CF contributed equally.

LW and CF are joint first authors.

Accepted 05 May 2026

For numbered affiliations see end of article.

Correspondence to
Li Yu; yuli@szu.edu.cn

Yisheng Li; ysli@haoshibio.com

ABSTRACT

Background Relapsed or refractory (R/R) B-cell non-Hodgkin's lymphoma (B-NHL) remains a major therapeutic challenge despite CD19-directed chimeric antigen receptor (CAR) T-cell therapies, with treatment failure often driven by antigen escape and limited CAR-T persistence. Dual targeting of CD19 and CD20 may mitigate antigen loss. We conducted an expanded phase I/II study of bispecific CD19/20 CAR-T cells and incorporated spatially resolved single-cell transcriptomics to evaluate tumor-intrinsic and microenvironmental factors of clinical response.

Methods Patients with R/R B-NHL received CD19/20 CAR-T cells following lymphodepletion. Efficacy, safety, CAR-T expansion/persistence, and B-cell reconstitution were assessed. Pretreatment tumor biopsies from five patients with divergent outcomes underwent spatial single-cell transcriptomic profiling.

Results 32 patients were treated, including 24 with diffuse large B-cell lymphoma. Among 31 evaluable patients, the best overall response rate was 74%, including 58% achieving complete remission. Median progression-free and overall survival were 6.8 and 22.1 months, respectively. Response rates were higher in patients with normal lactate dehydrogenase. CAR-T expansion peaked on days 7–17, and persistence exceeded 500 days in long-term responders. Cytokine release syndrome occurred in 53% (12% grade ≥3) and immune effector cell-associated neurotoxicity syndrome in 9% (all grade 3), with no lasting deficits. Spatial profiling identified two dominant tumor architectures: (1) a B-cell-dominant phenotype, in which durable remission was associated with heightened apoptotic competence in malignant B cells, and (2) a fibroblast-enriched and monocyte/macrophage-enriched phenotype, in which response correlated with a chemokine-rich, T-cell-permissive microenvironment.

Conclusions Bispecific CD19/20 CAR-T therapy produced durable clinical activity with manageable toxicity. Spatial single-cell analysis reveals distinct tumor-intrinsic and microenvironmental features associated with CAR-T responsiveness, providing a spatially informed framework for understanding heterogeneous therapeutic outcomes.

Trial registration number NCT04723914.

WHAT IS ALREADY KNOWN ON THIS TOPIC

⇒ CD19 chimeric antigen receptor (CAR)-T therapy is effective in relapsed or refractory B-cell non-Hodgkin's lymphoma, but treatment failure remains common due to antigen escape and limited CAR-T cell persistence.

WHAT THIS STUDY ADDS

⇒ Bispecific CD19/20 CAR-T cells demonstrate durable clinical activity with manageable toxicity, and spatial single-cell transcriptomics reveals that both tumor-intrinsic apoptotic competence and a T-cell-permissive microenvironment are key determinants of response.

HOW THIS STUDY MIGHT AFFECT RESEARCH, PRACTICE OR POLICY

⇒ Spatially informed profiling of tumor and microenvironmental features may guide patient stratification and the development of combination strategies to enhance CAR-T efficacy and durability.

INTRODUCTION

Diffuse large B-cell lymphoma (DLBCL) is the most common subtype of B-cell non-Hodgkin's lymphoma (B-NHL). Approximately 40% of patients develop refractory disease after initial therapy or relapse following remission. In patients ineligible for transplantation or relapsing after autologous transplantation, second-line therapy yields an overall response rate (ORR) of only 20–30% and a median overall survival (OS) of approximately 6 months.[1–3]

In recent years, five anti-CD19 chimeric antigen receptor (CAR)-T products have been approved globally for relapsed/refractory (R/R) large B-cell lymphoma (LBCL), follicular lymphoma (FL), or mantle cell

lymphoma (MCL). As ≥third-line therapy, reported ORRs in R/R B-NHL range from 53% to 97% (53–83% for LBCL, 86–97% for FL, and 83% for MCL), with complete response (CR) rates of 39–94% (39–58% for LBCL, 68–94% for FL, and 68% for MCL).[4–10] Despite these favorable outcomes, ~20% of patients with LBCL exhibit primary resistance, and 50–60% of B-NHL cases relapse,[11] often due to limited CAR-T persistence or antigen escape.[12–14] A potential strategy to prevent antigen escape is dual-antigen targeting. Tandem CARs against CD19 and CD22 have shown promising activity in R/R B-cell acute lymphoblastic leukemia.[15] We previously reported encouraging results from a phase I/II trial (n=11) of bispecific CD19/20 CAR-T cells in R/R B-NHL.[16]

To further validate these findings and explore factors contributing to heterogeneous responses, we expanded the original cohort and extended follow-up. In addition to comprehensive clinical analyses, we incorporated spatially resolved transcriptomic profiling of pretreatment tumor biopsies to examine tumor-intrinsic and microenvironmental features associated with response to bispecific CD19/20 CAR-T therapy.

MATERIALS AND METHODS

Patients and study design

This phase I/II, single-arm clinical trial was conducted at Shenzhen University General Hospital (May 2021 to November 2024) to evaluate the safety, efficacy, and biological correlates of bispecific CD19/20 CAR-T cell therapy in patients with R/R B-NHL. The study was approved by the institutional ethics committee, registered at ClinicalTrials.gov (NCT04723914), and conducted in accordance with the Declaration of Helsinki. Written informed consent was obtained from all participants.

Eligible patients met the following criteria: (1) age 14–75 years; (2) histological confirmation of CD19 and/or CD20 expression; (3) refractory or relapsed disease after prior therapy; and (4) Eastern Cooperative Oncology Group performance status ≤2. One 76-year-old patient was enrolled with prior approval from the institutional ethics committee before enrollment. Diagnoses were based on the 2008 WHO classification, including DLBCL, transformed FL (tFL), MCL, FL, primary mediastinal large B-cell lymphoma, and Burkitt lymphoma.

CAR-T cell manufacturing and lymphodepletion

The bispecific anti-CD19/CD20 CAR incorporated CD20 (Leu16) and CD19 (FMC63) single-chain variable fragments (scFvs) linked to CD8 hinge and transmembrane domains and 4-1BB/CD3ζ signaling domains. Heavy and light chains were connected via $(GGGGS)_3$ and 218s linkers. CAR-T cells were manufactured as described previously.[16]

All patients received lymphodepleting chemotherapy with fludarabine (30 mg/m²/day×3 days) and cyclophosphamide (300 mg/m²/day×3 days). Fresh CAR-T products were infused at 0.3–2.6×10⁶ CAR-T cells/kg.

Toxicity and efficacy assessment

Primary objectives were safety and ORR, defined by 2014 Lugano criteria.[17] Cytokine release syndrome (CRS) and immune effector cell-associated neurotoxicity syndrome (ICANS) were graded using American Society for Transplantation and Cellular Therapy consensus criteria.[18] Tocilizumab or dexamethasone was administered as indicated. Secondary objectives included duration of response (DOR), progression-free survival (PFS), and OS. Exploratory analyses included CAR-T cell expansion/persistence, and peripheral B-cell recovery. B-cell reconstitution was defined as ≥1% $CD19^+$ B cells among peripheral lymphocytes by flow cytometry. CAR-T expansion and persistence were quantified using multiparameter flow cytometry.

Spatial transcriptomics

Pretreatment tumor biopsies from five patients with divergent outcomes underwent spatial transcriptomic profiling using the 10x Genomics Visium HD platform. Raw sequencing data were processed with Space Ranger (V.3.0) and aligned to GRCh38. Quality control was performed using the Seurat package (V.5.0) in R (V.4.3). Spots with <200 detected genes or >20% mitochondrial content were excluded; genes detected in <10 spots were removed.

Data normalization employed SCTransform with variance stabilization. Samples were integrated using reciprocal principal component analysis (RPCA) with Seurat's FindIntegrationAnchors (reduction="rpca", dims=1:30), followed by IntegrateData to correct batch effects while preserving biological variation.

Dimensionality reduction was performed using principal component analysis (top 30 principal components [PCs]) and Uniform Manifold Approximation and Projection. Cell clusters were identified using shared nearest neighbor clustering (resolution=0.8) and annotated based on canonical markers and reference single-cell RNA sequencing datasets.

Differential gene expression and functional enrichment analysis

Differential expression analysis was performed using Seurat's FindMarkers (Wilcoxon rank-sum test), with significance defined as adjusted $p<0.05$ and $|\log_2 FC|>0.25$. Genes identified by Seurat's FindMarkers analysis were subsequently subjected to Gene Ontology (GO) analysis.

Spatial neighborhood analysis

Spatial co-occurrence between cell types was computed using squidpy.gr.co_occurrence across 20 distance bins (0–30% of maximum spatial range). Co-occurrence ratio >1 indicated spatial attraction; <1 indicated repulsion.

Statistical analysis

All statistical analyses were conducted using GraphPad Prism (V.10.5.0), R (V.4.3) and Python (V.3.10). Continuous variables are reported as medians with ranges, and categorical variables as frequencies with percentages.

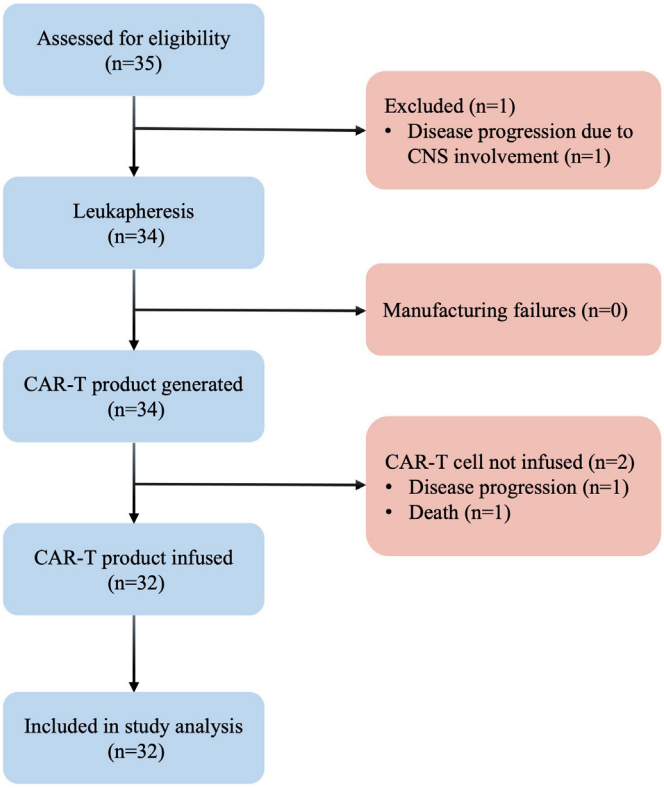

Figure 1 Study diagram. CAR, chimeric antigen receptor. CNS, central nervous system.

Comparisons between groups were conducted using the Wilcoxon rank-sum test for continuous variables and Fisher's exact test for categorical variables. Kaplan-Meier analysis was used to estimate DOR, PFS, and OS. Best overall response rates were visualized using forest plots with corresponding 95% CIs. All statistical tests were two-sided, and $p<0.05$ was considered statistically significant.

RESULTS

Patient characteristics

Between May 2021 and November 2024, 35 patients were screened, 34 underwent leukapheresis, and 32 patients with NHL meeting inclusion criteria received anti-CD19/20 CAR-T therapy (figure 1). The median age was 56 years (range: 28–76), with 15 males (47%) and 17 females (53%). Baseline demographics and clinical characteristics are summarized in table 1.

Histological subtypes included DLBCL (n=24, 75%; germinal center B-cell (GCB) or non-GCB), tFL (n=3, 9%), MCL (n=2, 6%), and one case each of FL, primary mediastinal B-cell lymphoma, and Burkitt lymphoma (n=3, 9%). One patient (3%) had previously received CD19 CAR-T therapy. Most patients (94%) had stage III–IV disease; 62% (n=20) had International Prognostic Index (IPI) scores ≥3. 24 patients (75%) had refractory disease and 8 (25%) had relapsed disease. 13 (41%) were double-expressor lymphomas (c-MYC with BCL2 or BCL6), and 72% had Ki-67≥70%. Extranodal involvement was present in 84%, and more than half had elevated

Table 1 Baseline characteristics

	Patients (N=32), no (%)
Age (years)	
Median (range), years	56 (28–76)
≥60	12 (38)
Sex	
Male	15 (47)
Female	17 (53)
Predominant histology	
DLBCL	24 (75)
tFL	3 (9)
Others (MCL, FL, PMBCL, BL)	5 (16)
Cell of origin in DLBCL	
GCB	8 (25)
Non-GCB	16 (50)
Disease stage at enrollment	
II	2 (6)
III	4 (13)
IV	26 (81)
IPI at enrollment	
<3	12 (38)
≥3	20 (62)
Previous response status	
Refractory to last line	24 (75)
Relapsed to last line	8 (25)
ECOG at enrollment	
0–1	20 (63)
2	12 (37)
Number of previous lines of anti-neoplastic therapy	
≤2 lines	8 (25)
>2 lines	24 (75)
IHC (CD19, CD20)	
CD20+	31 (97)
CD19+	30 (94)
CD19–	2 (6)
CD20–	1 (3)
Double or triple expression: MYC plus BCL2, BCL6 or both	
Yes	13 (41)
No	12 (38)
Miss data	7 (21)
Ki-67	
<70%	8 (25)
≥70%	23 (72)
NA	1 (3)
Extranodal involvement	

Continued

Table 1 Continued

	Patients (N=32), no (%)
Yes	27 (84)
No	5 (16)
Elevated LDH at enrollment	
Yes	18 (56)
No	14 (44)

Data presented as no, (%).
BL, Burkitt lymphoma; DLBCL, diffuse large B-cell lymphoma; ECOG, Eastern Cooperative Oncology Group performance status; GCB, germinal center B-cell-like; IHC, immunohistochemistry; IPI, International Prognostic Index; Ki-67, Ki-67 proliferation index; LDH, lactate dehydrogenase; MCL, mantle cell lymphoma; NA, not available; PMBCL, primary mediastinal B-cell lymphoma; tFL, transformed follicular lymphoma.

lactate dehydrogenase (LDH). 29 patients had confirmed dual CD19/CD20 expression by immunohistochemistry.

Response and survival

All patients received lymphodepleting chemotherapy before CAR-T infusion. The median infused CAR-T dose was 1.0×10^6 cells/kg (range: 0.3–2.6). 1 patient (Case 3) died before the first response evaluation; thus, 31 patients were evaluable for efficacy. The best ORR was 74% (23/31); 18 patients (58%) achieved CR and 5 (16%) achieved partial remission (PR). The median time to first response was 1.5 months (range: 0.9–3.4), and the median time to first CR was 2.6 months (range: 1.0–9.5) (figure 2A; table 2).

The median DOR was 19.5 months (95% CI 10.7 to 38.4) (figure 2B; table 2). The longest observed response was 38.8 months (Case 4). Among patients who achieved CR, the median follow-up was 16.9 months, and the median DOR was not reached; the 12-month probability of

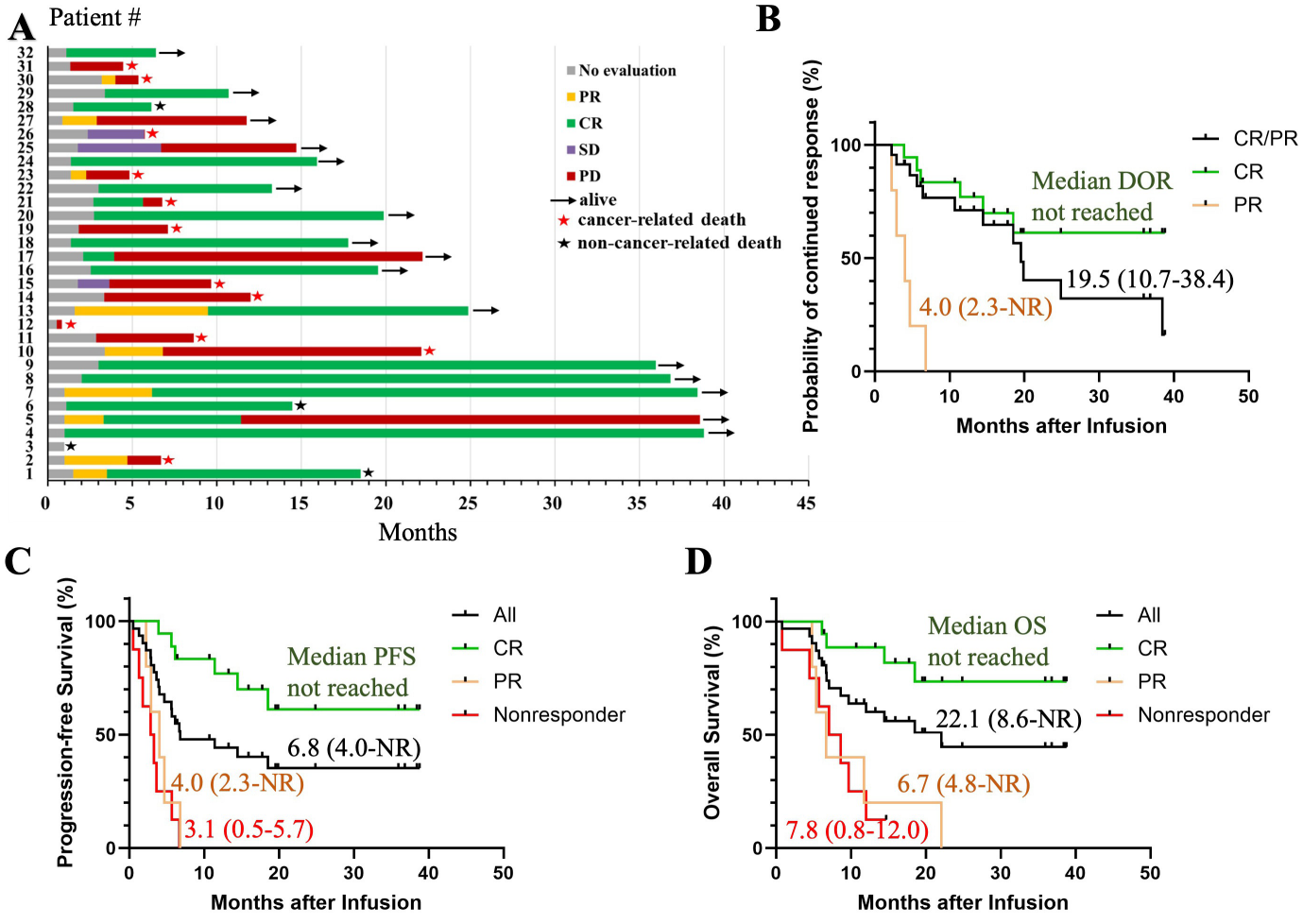

Figure 2 Clinical outcomes. (A) Clinical response among 32 patients. (B) Probability of continued response (%). (C) PFS probability. (D) OS probability. Outcomes are stratified by best response. CR, complete remission; DOR, duration of response; NR, not reached; OS, overall survival; PD, progressive disease; PFS, progression-free survival; PR, partial remission; SD, stable disease.

Table 2 Patient best responses

	Patients (n=31)
Best overall response	23 (74%)
Complete response	18 (58%)
Partial response	5 (16%)
Stable disease	3 (10%)
Progressive disease	4 (16%)
Continued response	15 (48%)
Progression following complete response	3 (10%)
Median time to first response, months	1.5 (0.9–3.4)
Median time to first CR, months	2.6 (1.0–9.5)
Median duration of response, months (95% CI)	19.5 (10.7 to 38.4)
Probability of continued response at 12 months (95% CI), %	52.2 (33.0 to 70.8)
Median PFS, months (95% CI)	6.8 (4.0 to NR)
Probability of PFS at 12 months (95% CI), %	38.7 (23.7 to 56.2)
Median OS, months (95% CI)	22.1 (8.6 to NR)
Median follow-up, months (95% CI)	13.3 (7.1 to 19.5)
Probability of OS at 12 months (95% CI), %	54.8 (37.8 to 70.8)

CR, complete response; NR, not reached; OS, overall survival; PFS, progression-free survival.

continued response was 52.2% (95% CI 33.0% to 70.8%). All PR patients (n=5) progressed within a median of 4.0 months (range: 2.3–6.8). Among CR patients (n=18), 15 remained in remission, while 3 relapsed at a median of 5.6 months (range: 3.9–11.4). Biopsies from the two relapsed cases confirmed retained CD19 and CD20 expression.

In the overall cohort, the median follow-up was 13.3 months (95% CI 7.1 to 19.5). Median PFS was 6.8 months (95% CI 4.0 to not reached [NR]) and median OS was 22.1 months (95% CI 8.6 to NR). The 12-month PFS and OS rates were 38.7% (95% CI 23.7% to 56.2%) and 54.8% (95% CI 37.8% to 70.8%), respectively. Median PFS and OS were not reached in patients achieving CR (figure 2C and D).

Response rates were not significantly associated with baseline demographic or disease characteristics, infused dose, or prior treatment history. In exploratory subgroup analyses, ORR was nominally higher in patients with normal LDH (93%; 95% CI 69% to 99%) compared with those with elevated LDH (58%; 95% CI 36% to 78%; p=0.045) (figure 3).

Safety and adverse events

A total of 32 patients received CD19/20 CAR-T cell products. 17 patients (53%) developed CRS with a median onset of 2 days post-infusion (range: 0–16) and median duration of 3 days (range: 1–8) (online supplemental Table 1). CRS was grade 1 or 2 in 13 patients (41%) and grade 3 or 4 in 4 (12%), presenting with fever, hypotension, and severe hypoxemia. Three patients (9%) developed grade 3 ICANS, with a median onset of 16 days (range: 6–22) post-infusion, and median duration of 1 day. Both CRS and ICANS were managed per institutional guidelines. Seven patients (22%) received tocilizumab (median two doses, range: 1–6), and four (13%) received dexamethasone. No persistent neurological deficits were observed in the cohort.

Key grade 3 or higher adverse events included: fatigue (n=3, 9%), edema (n=1, 3%), hyponoia (n=1, 3%), increased alanine aminotransferase (ALT) or aspartate aminotransferase (AST) (n=3, 9%), hypokalemia (n=2, 6%), anemia (n=10, 31%), neutrophil count decreased (n=24, 75%), platelet count decreased (n=11, 34%), anorexia (n=2, 6%), nausea (n=1, 3%), upper respiratory infection (URI) (n=2, 6%), lung infection (n=5, 16%), skin infection (n=1, 3%), sepsis (n=3, 9%), sinus tachycardia (n=1, 3%), heart failure (n=1, 3%), and musculoskeletal disorders (n=2, 6%). One patient died of severe pneumonia (pulmonary infection) before the first response evaluation and was recorded as having a grade 5 lung infection. This patient also experienced grade 3 CRS, which was managed with tocilizumab. The primary cause of death was severe pneumonia and was considered unrelated to CAR-T therapy.

CAR-T cell expansion, persistence and B-cell recovery

CAR-T expansion peaked during days 7–17 post-infusion, with a median peak of 81.5 cells/µL (range: 0.35–1127) (figure 4A and online supplemental Figure 1). No statistically significant differences in peak CAR-T expansion were observed between responders and non-responders or between patients with durable CR and those who relapse (figure 4B and C).

As of the last available data, CAR-T cells remained detectable via flow cytometry in 11 of 15 patients with ongoing CR, with the longest persistence reaching 551

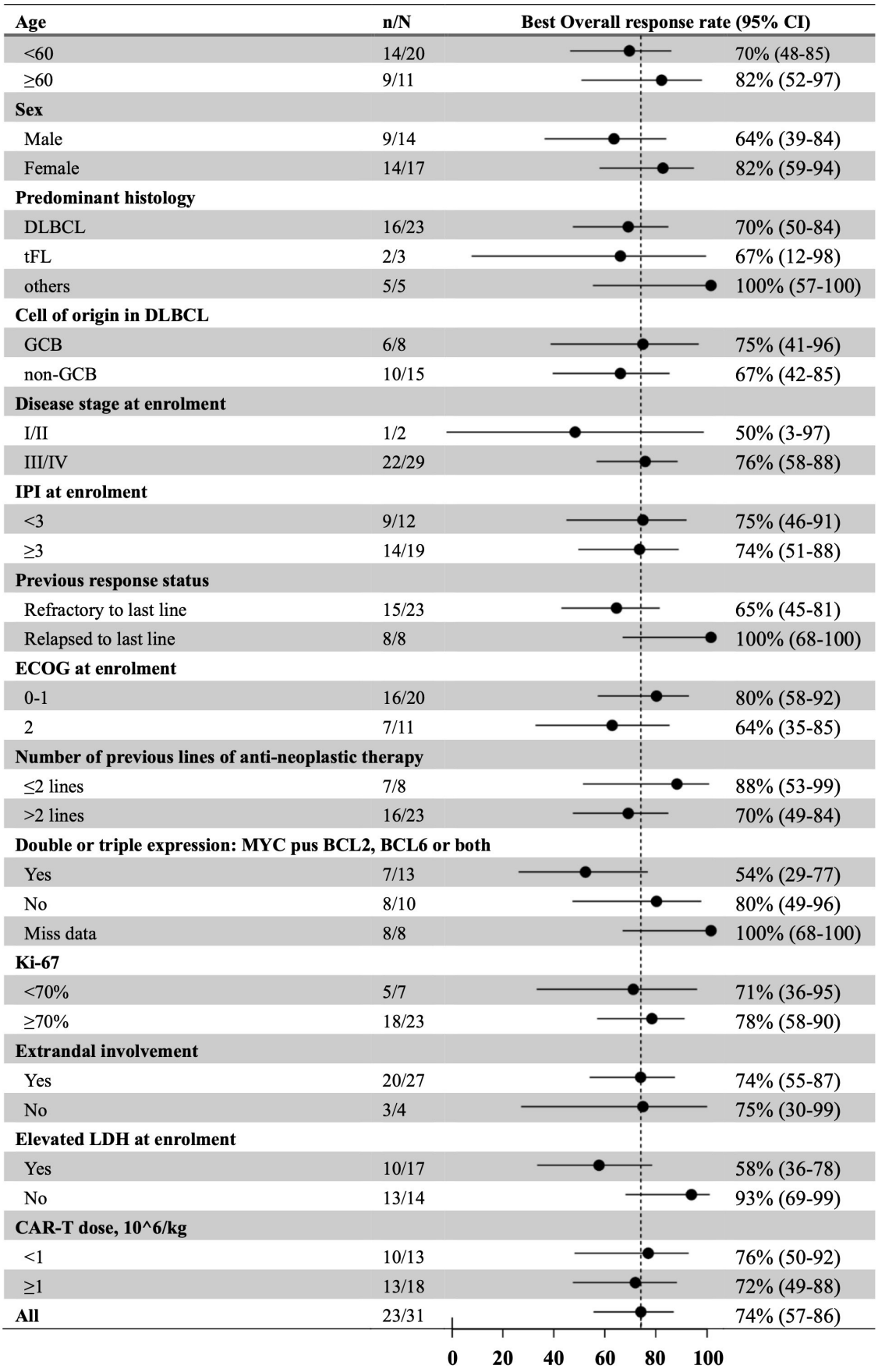

Figure 3 Best overall response rate by subgroup. CAR, chimeric antigen receptor; DLBCL, diffuse large B-cell lymphoma; ECOG, Eastern Cooperative Oncology Group performance status; GCB, germinal center B-cell-like; IPI, International Prognostic Index; Ki-67, Ki-67 proliferation index; LDH, lactate dehydrogenase; tFL, transformed follicular lymphoma.

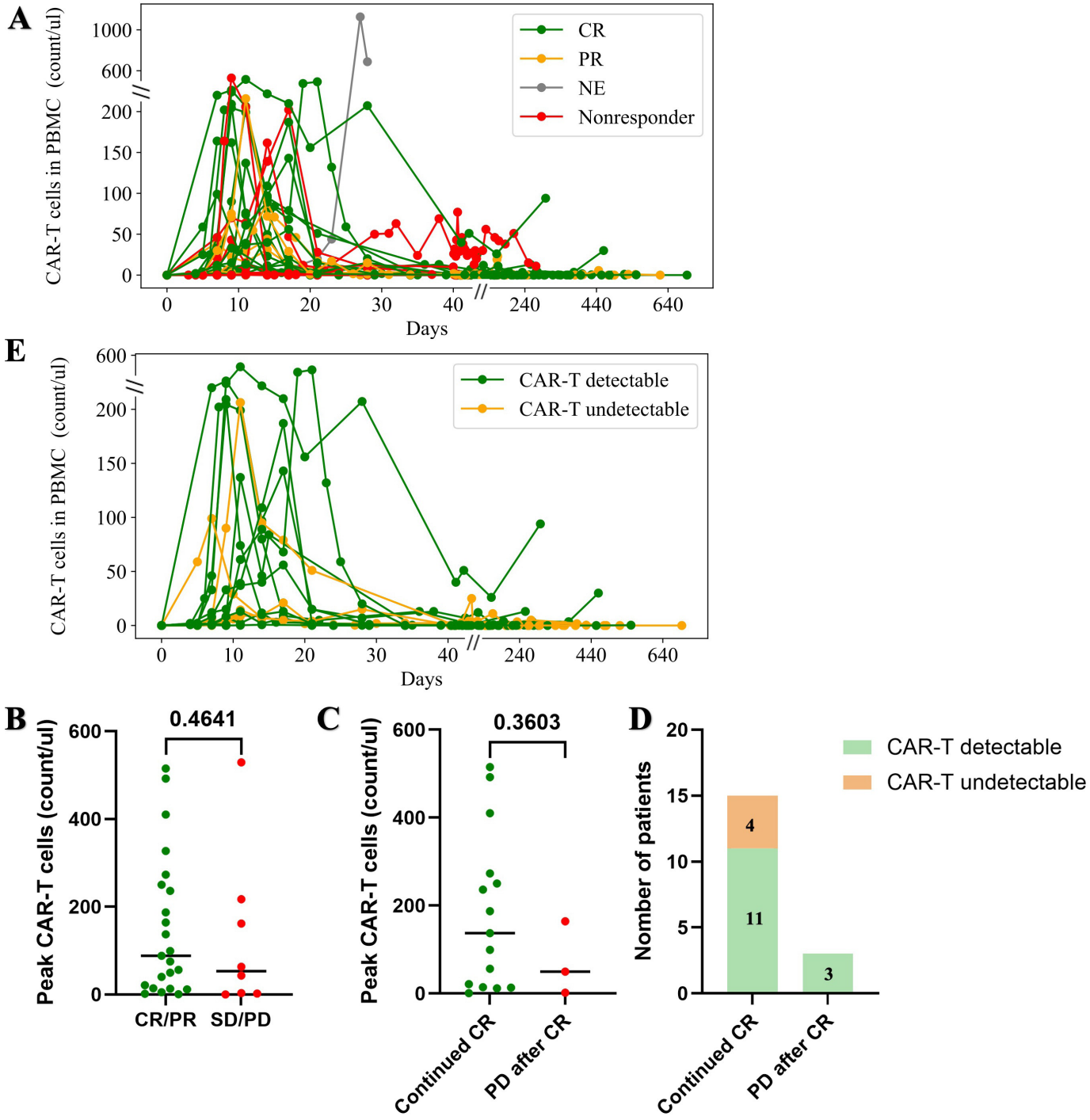

Figure 4 CAR-T cell pharmacokinetics. (A) CAR-T cell counts in PBMCs, measured by flow cytometry and color-coded by best response. (B) Peak CAR-T cell expansion in responders (CR/PR; n=23) versus non-responders (SD/PD; n=8). Median values and p value shown. (C) Peak CAR-T cell expansion in patients with continued CR (n=15) versus those with PD after CR (n=3). Median values and p value shown. (D) Number of patients with detectable versus undetectable CAR-T cells at end of follow-up, stratified by group. (E) CAR-T cell counts in PBMCs among patients with continued CR in two groups based on whether CAR-T could be detected at the final follow-up. CAR, chimeric antigen receptor; CR, complete remission; NE, no evaluation; PBMC, peripheral blood mononuclear cell; PD, progressive disease; PR, partial remission; SD, stable disease.

days post-infusion (the maximum in this trial by the cut-off date). CAR-T cells were also detectable in three patients with disease relapse, with no significant difference between the two groups (figure 4D and E, p>0.9999, Fisher's exact test).

Peripheral blood B cells became undetectable in all patients following CAR-T cell infusion. $CD19^{+}$ B-cell recovery occurred in 11 patients (34%), with a median time of 179 days (range: 61–473 days) post-infusion (online supplemental Figure 2A). No significant

association between B-cell recovery and disease status was observed in this cohort; the corresponding data are shown in online supplemental Figure 2B and C.

B-NHL exhibits spatially distinct cellular architectures

To identify determinants of clinical response to CAR-T cell therapy in B-NHL, we stratified the 32 enrolled patients into two predefined subgroups: those achieving long-term complete remission (LtCR; remission >1 year) and non-responders (nonR; best response of PD or SD). Baseline clinical characteristics were generally comparable between the LtCR and nonR groups, with no statistically significant differences observed (online supplemental Table 2).

To further explore tumor-intrinsic and microenvironmental factors that may influence CAR-T efficacy, we performed spatially resolved single-cell transcriptomics on pretreatment tumor biopsies from five patients with divergent clinical outcomes, as summarized in online supplemental Table 3. Three patients subsequently achieved LtCR (P1.1, P1.2, P1.3), whereas two patients were classified as nonR (P2.2, P2.3). After stringent quality filtering, a total of 35,759 high-quality cells were retained for downstream analysis. Unsupervised clustering resolved six major cell populations, including B cells, myeloid-like B cells, plasma cells, fibroblasts, monocyte/macrophage (Mono/Mϕ), and endothelial cells (figure 5A and B).

Spatial mapping demonstrated that the five samples segregated into two dominant architectural phenotypes: (1) B-cell-dominant type (P1.1, P1.3, P2.3), characterized by dense malignant B-cell infiltrates; and (2) fibroblast-enriched and Mono/Mϕ-enriched type (P1.2, P2.2), marked by extensive stromal and myeloid remodeling. These transcriptomic classifications were concordant with the histopathological features observed on H&E staining (figure 5C and D).

Apoptotic competence of malignant B cells prior to CAR-T infusion correlates with treatment response in B-cell-dominant B-NHL

Within the B-cell-dominant subgroup, differential gene expression analyses comparing LtCR and nonR patients revealed a transcriptional program strongly associated with apoptotic susceptibility in responders. LtCR samples exhibited higher expression of multiple pro-apoptotic genes (eg, *CASP3*, *CASP9*, *BAK1*, *CIDEB*) and downregulation of anti-apoptotic genes such as *BCL2L2* and *AKT1* (figure 6A).

GO enrichment confirmed significant activation of pathways related to intrinsic apoptotic signaling and apoptotic regulation, including regulation of response to DNA damage stimulus, IκB kinase/NF-κB signaling, regulation of protein ubiquitination, and protein monoubiquitination (figure 6B). Collectively, these findings suggest that a pre-existing pro-apoptotic molecular state in malignant B cells may be associated with greater sensitivity to CAR-T cytotoxicity.

Chemokine-driven immune microenvironment prior to CAR-T infusion predicts response in fibroblast-dominant and Mono/Mϕ-dominant B-NHL

In the fibroblast-dominant and Mono/Mϕ cell-dominant subgroup, differential expression analyses of non-B-cell compartments (fibroblasts, Mono/Mϕ cells, endothelial cells) revealed markedly elevated chemokine expression in the LtCR sample compared with the nonR sample. Upregulated chemokines included *CCL5*, *CCL17*, *CCL22*, *CXCL9*, *CXCL10*, and *CXCL12* (figure 7A). Dot-plot visualization further demonstrated that these chemokines were predominantly produced by Mono/Mϕ cells (figure 7B). Consistently, GO biological process enrichment analysis of cell type-specific differentially expressed genes between P1.2 and P2.2 highlighted pathways related to immune activation, leukocyte migration, and chemotaxis (online supplemental Table 4).

Spatial neighborhood (co-occurrence) analysis revealed that T cell-recruiting chemokines (*CCL5*, *CXCL9*, *CXCL10*) were spatially colocalized with Mono/Mϕ populations, whereas fibroblasts, endothelial cells, and malignant B cells were distributed at greater distances from these chemokine-rich regions (figure 7C). This pattern indicates that, in addition to lymphoma-fibroblast interactions, the presence of a pre-existing immunostimulatory niche-driven largely by chemokine-producing Mono/Mϕ cells—may facilitate T-cell recruitment and activation, thereby contributing to favorable CAR-T therapeutic responses.

Collectively, these analyses define two spatially distinct tumor architectures in B-NHL associated with divergent mechanisms of response to CD19/20 CAR-T therapy. In B-cell-dominant tumors, therapeutic efficacy appears to be linked to tumor-intrinsic apoptotic competence of malignant B cells, whereas in fibroblast-enriched and Mono/Mϕ-enriched tumors, response is associated with microenvironmental immunologic accessibility mediated by chemokine-rich niches that promote CAR-T cell recruitment. Non-responding tumors within each architecture lack these respective features, exhibiting impaired apoptotic priming or deficient chemokine-mediated immune recruitment. This architecture-specific framework provides a unified interpretation of the spatial transcriptomic findings summarized in figure 8.

DISCUSSION

Recently, considerable efforts have focused on developing CARs that target multiple antigens to overcome CD19 antigen escape observed in CD19 CAR-T trials. CD20 is an attractive target for B-cell malignancies, as it is broadly expressed on mature B cells but absent from hematopoietic stem cells.[19] In our previous work, we engineered a tandem CAR incorporating scFvs against both CD19 and CD20, which demonstrated potent antitumor activity in vitro. We also reported promising outcomes in an initial phase I/II trial (n=11) of this bispecific CAR-T in patients with R/R B-cell malignancies.[16]

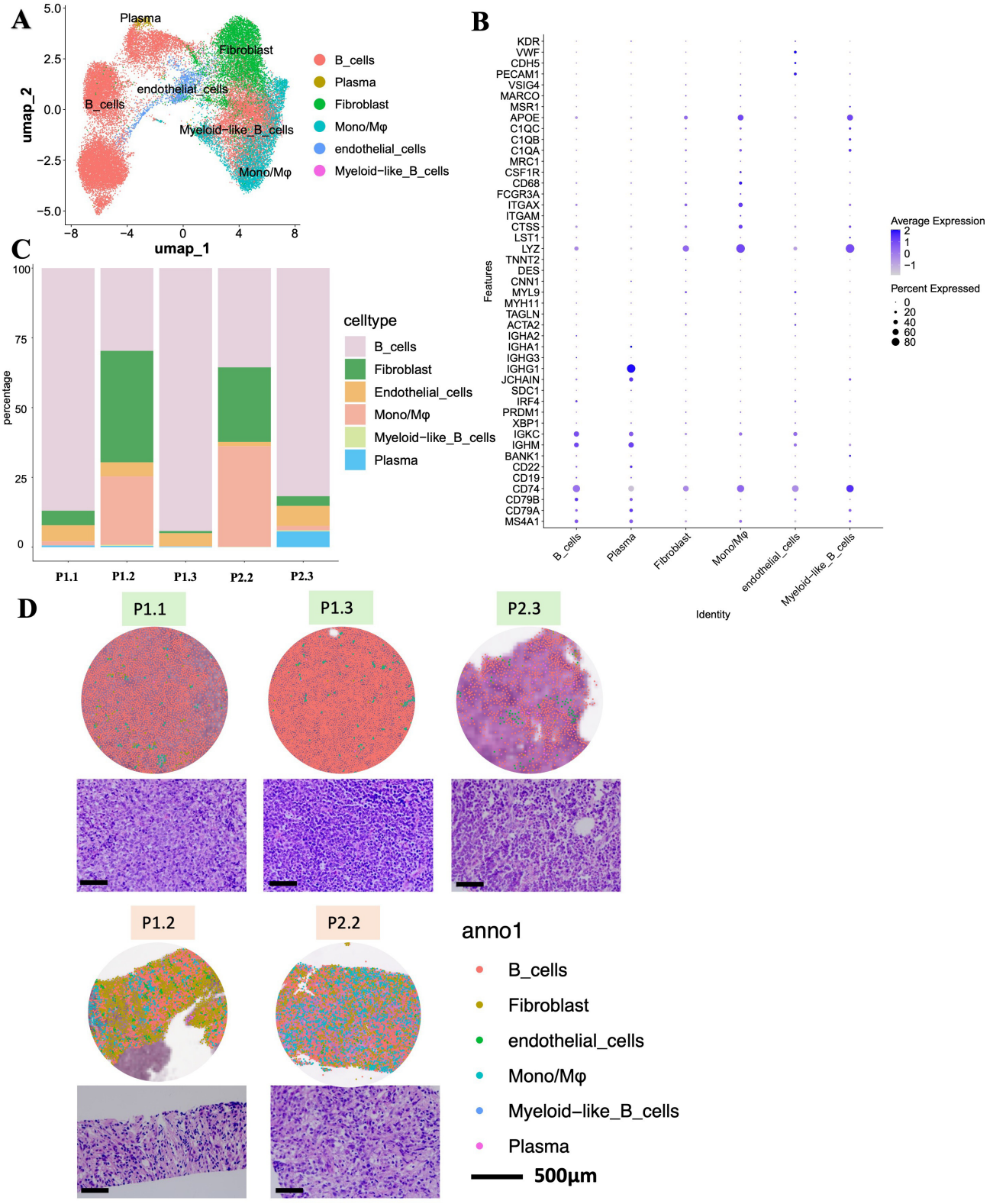

Figure 5 Spatially distinct cellular architectures identified by single-cell spatial transcriptomics in B-cell non-Hodgkin's lymphoma. (A) UMAP visualization of 35,759 single cells derived from pretreatment tumor biopsies of five patients with divergent clinical outcomes (three long-term complete responders and two non-responders). Cells cluster into major populations annotated as malignant B cells, myeloid-like B cells, plasma cells, fibroblasts, monocyte/macrophage cells, and endothelial cells. (B) Dot plot showing canonical marker expression across annotated cell populations, with color indicating average expression and dot size indicating the proportion of expressing cells. (C) Relative proportions of major cell types across individual pretreatment tumor biopsies. (D) Representative spatial cell-type maps and corresponding H&E-stained sections derived from the same tumor specimens (spatial maps: scale bar, 500 μm; original magnification×1.2; H&E: scale bar, 50 μm; original magnification×40). UMAP, Uniform Manifold Approximation and Projection.

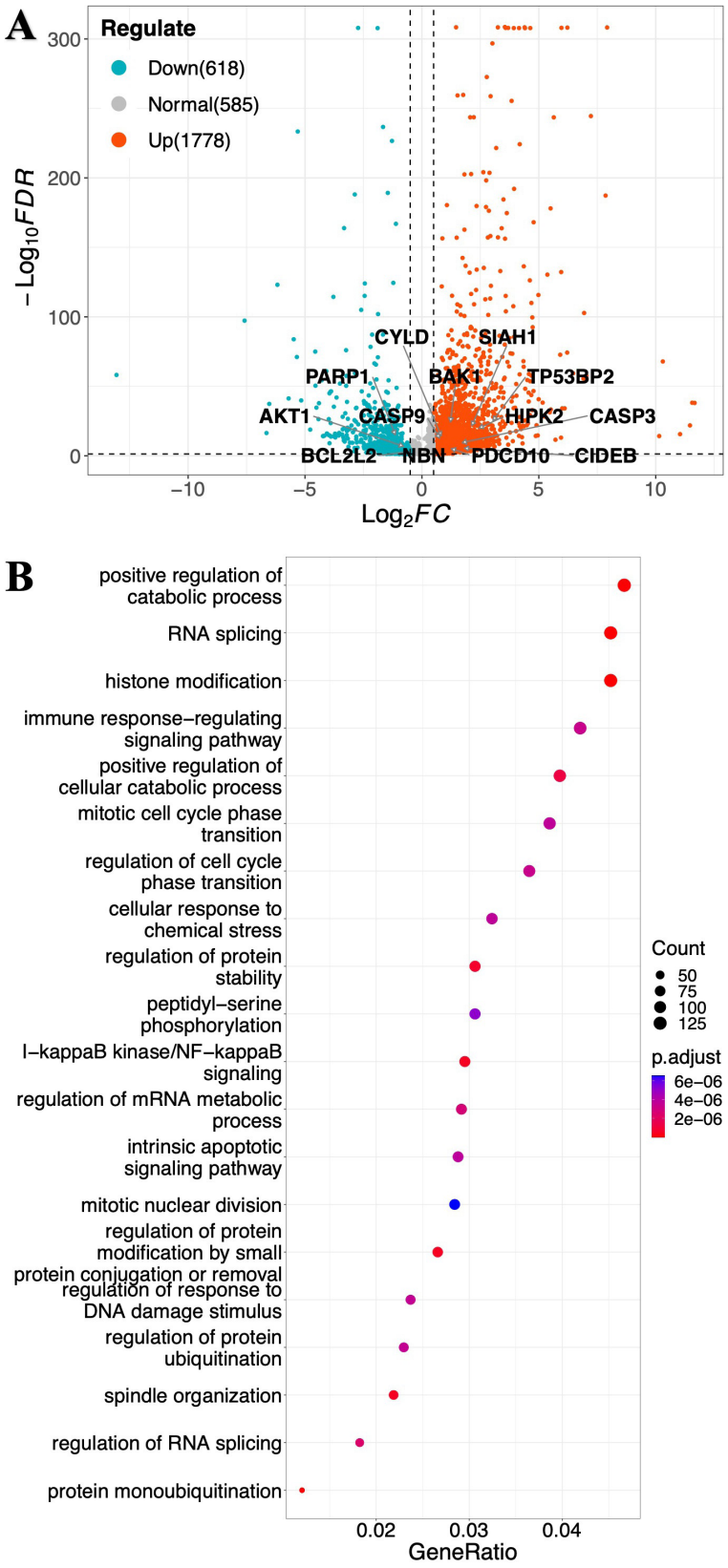

Figure 6 Apoptotic gene programs in malignant B cells associate with response to CAR-T therapy in B-cell-dominant B-NHL. (A) DEGs in malignant B cells between long-term complete responders (P1.1 and P1.3) and non-responders (P2.3) prior to CAR-T infusion. (B) Gene Ontology biological process enrichment analysis of DEGs. B-NHL, B-cell non-Hodgkin's lymphoma; CAR, chimeric antigen receptor; DEGs, differentially expressed genes; FDR, false discovery rate; mRNA, messenger RNA.

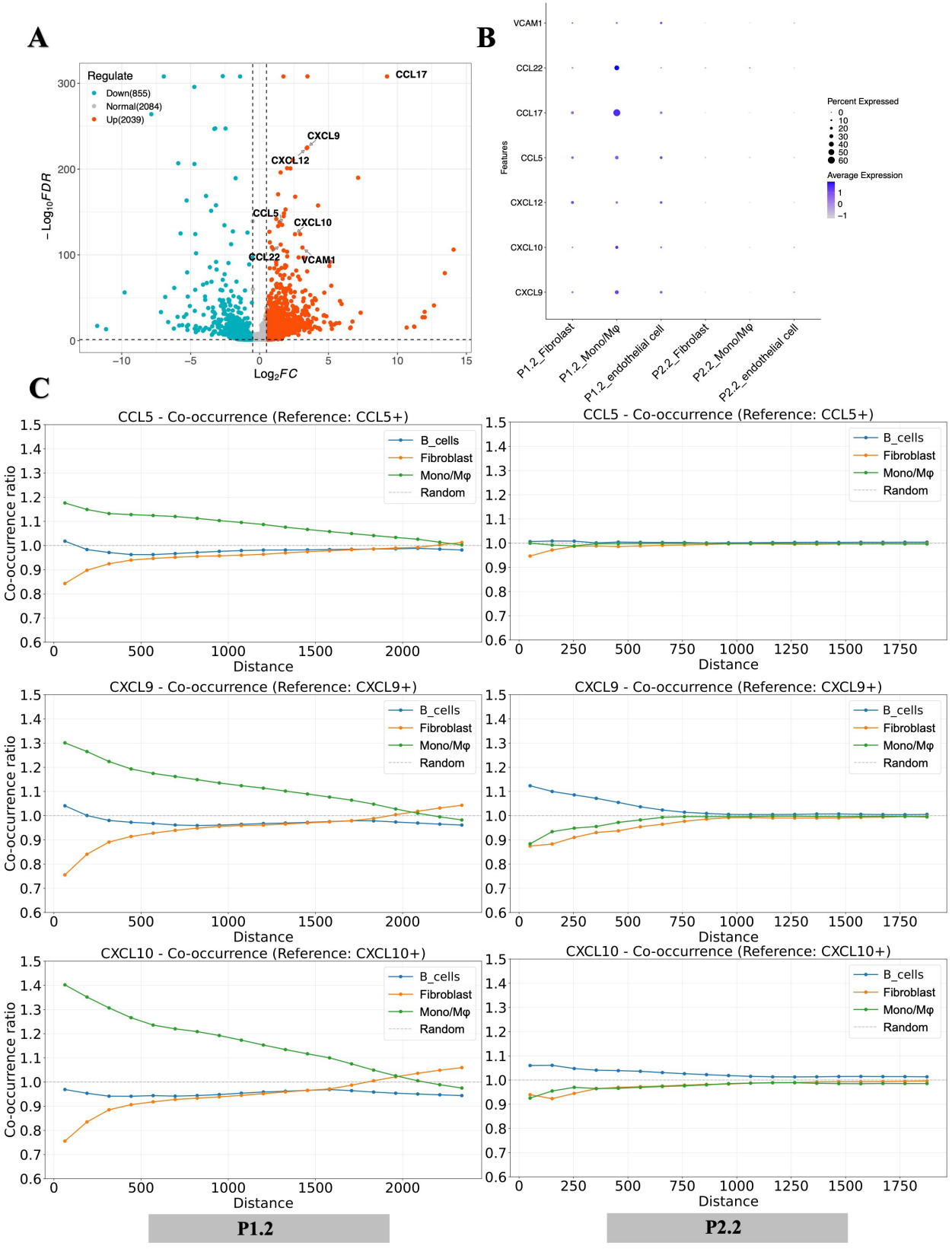

Figure 7 Chemokine-driven monocyte/macrophage niches associate with CAR-T response in fibroblast-enriched and monocyte/macrophage-enriched B-NHL. (A) Differentially expressed genes in non-B-cell compartments between an LtCR (P1.2) and a nonR (P2.2) prior to CAR-T infusion. (B) Dot plot showing expression levels and cellular distribution of key chemokines and lineage markers across major cell populations. (C) Spatial co-occurrence analysis of chemokine-expressing regions ($CCL5^+$, $CXCL9^+$, $CXCL10^+$) relative to monocyte/macrophage, malignant B-cell, and fibroblast populations as a function of distance in a representative LtCR (P1.2; left) and nonR (P2.2; right). B-NHL, B-cell non-Hodgkin's lymphoma; CAR, chimeric antigen receptor; FDR, false discovery rate; LtCR, long-term complete responder; nonR, non-responder.

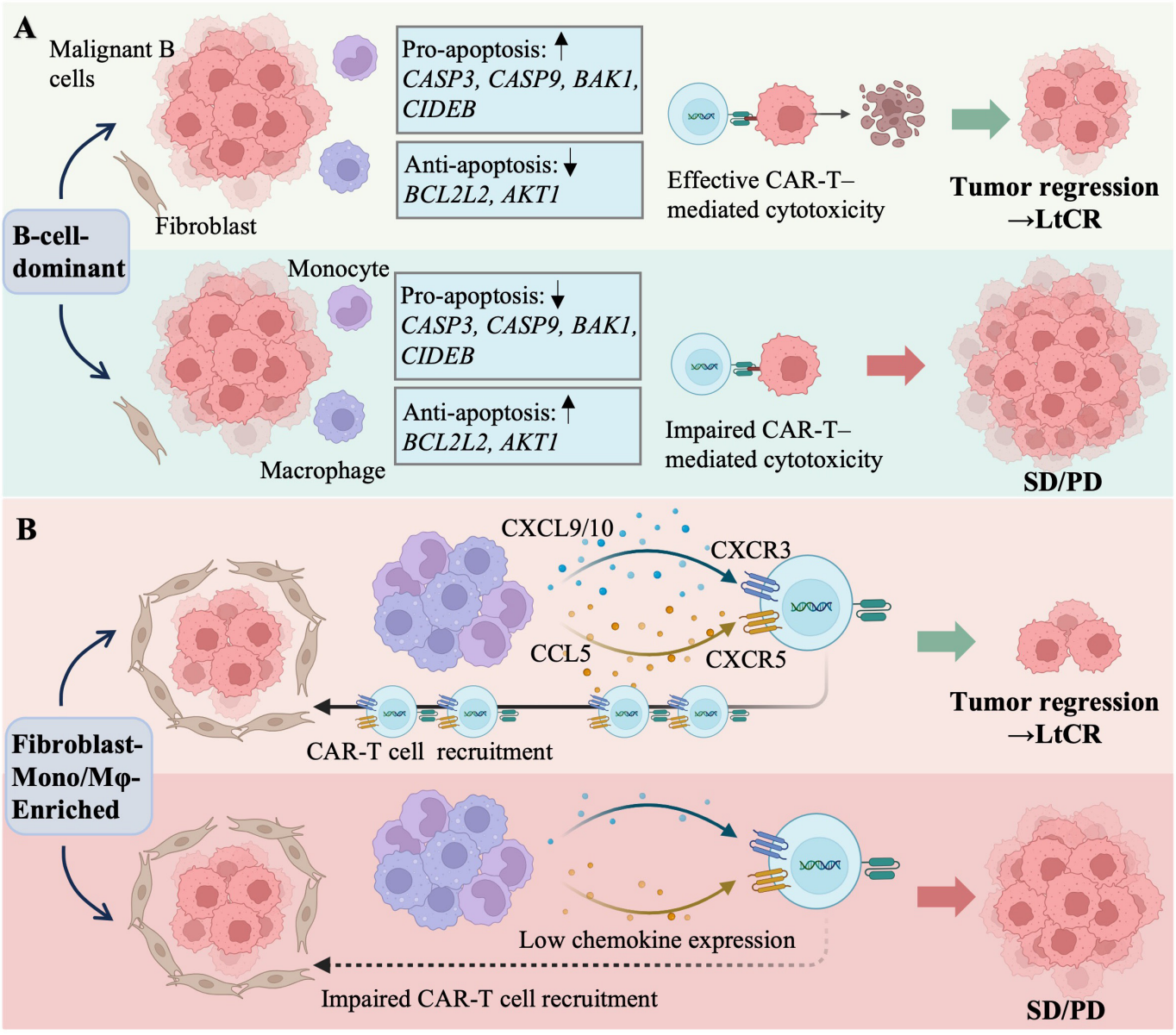

Figure 8 Schematic model of spatial tumor architectures associated with CAR-T response in B-cell non-Hodgkin's lymphoma. (A) B-cell-dominant architecture. Tumors segregate into responder and non-responder phenotypes, with LtCR exhibiting enhanced intrinsic apoptotic competence of malignant B cells, enabling effective CAR-T-mediated cytotoxicity, whereas non-responders display reduced apoptotic priming and impaired CAR-T efficacy. (B) Fibroblast-enriched and monocyte/macrophage (Mono/Mϕ)-enriched architecture. LtCR tumors are characterized by a chemokine-rich, T-cell-permissive microenvironment driven predominantly by Mono/Mϕ-derived chemokines (eg, CCL5, CXCL9, CXCL10), facilitating CAR-T recruitment and engagement, while non-responders lack such immunostimulatory niches. CAR, chimeric antigen receptor; LtCR, long-term complete responder; PD, progressive disease; SD, stable disease.

Here, we sought to validate those findings and explore covariates influencing clinical response. The therapy showed encouraging activity, with a best ORR of 74% and a CR rate of 58%. At data cut-off, 48% of patients remained in CR. Median DOR among responders was 19.5 months. For the overall cohort, median PFS and OS were 6.8 months and 22.1 months, respectively.

Among Food and Drug Administration-approved CD19 CAR-T products, reported ORRs were 83% with axicabtagene ciloleucel,[4] 73% with lisocabtagene maraleucel,[5] 53% with tisagenlecleucel,[6] and 78% with relmacabtagene autoleucel,[20] with corresponding CR rates of 58%, 53%, 39%, and 53%, respectively. Reported median PFS and OS have ranged from 2.9 to 7.0 months and from 11.1 to 27.3 months, respectively. Notably, the median duration of CR in TRANSCEND NHL 001[5] and ZUMA-1(4) was 26.2–62.2 months, with ongoing CR rates of 30% in ZUMA-1 and RELIANCE.[4 20] At a median follow-up of 16.9 months for patients achieving CR, the median DOR for CR patients in our study was not reached, and the ongoing CR rate was 48%. While these results appear favorable, longer follow-up is needed for confirmation.

In recent international studies of CD19/20 CAR-T therapy,[19 21–23] ORRs ranged from 79% to 92% and CR rates from 64% to 85%, broadly consistent with the outcomes observed in our study. Reported median PFS values in international CD19/20 CAR-T studies ranged from 15.6 to 27.6 months, numerically longer than those observed in our cohort, which may in part reflect differences in baseline risk profiles, including disease stage and IPI distribution. Reported relapse rates in these studies ranged from 18% to 27%, whereas relapse occurred in 3 of 31 evaluable patients in our study. Other bispecific strategies, particularly CD19/CD22-directed CAR-T cells, have also been explored in lymphoma. In published CD19/CD22 CAR-T studies, best ORRs ranged from 62% to 66% and CR rates from 29% to 49%.[24 25] In the ALEXANDER study, median PFS and OS were 3.32 and 13.8 months, respectively.[25] Collectively, these data suggest that dual-target CAR-T strategies beyond CD19/CD20 are also clinically active in lymphoma, although durability remains variable across constructs and studies.

In exploratory subgroup analyses, normal LDH was nominally associated with a higher response rate. This finding is consistent with previous reports linking elevated LDH before lymphodepletion or CAR-T infusion to inferior outcomes in B-NHL, likely reflecting greater tumor burden and more aggressive disease biology.[26–28] However, given the multiple subgroup comparisons in our study, this finding should be considered exploratory rather than definitive. Several retrospective studies have further suggested that disease debulking and LDH reduction before infusion may be associated with improved CAR-T outcomes.[26 29 30] Nevertheless, the current evidence remains largely retrospective, and prospective validation is warranted.

In pivotal trials of CD19 CAR-T therapies,[4–6 20] CRS occurred in 42–94% of patients, with grade ≥3 CRS reported in 2–23%; neurologic events occurred in 20–64% (grade ≥3: 5–30%). For CD19/20 CAR-T trials,[19 21–23] CRS rates were 64–94% (grade ≥3: 2–10%) and ICANS rates 6–32% (grade ≥3: 0–14%). In our study, CRS occurred in 53% of patients, with 12% experiencing grade 3–4 events, while ICANS occurred in 9% (all grade 3). These findings are consistent with international data and indicate a manageable safety profile for CD19/20 CAR-T therapy.

CD19-negative relapse has been reported in ~30% of evaluable post-relapse biopsy specimens after axicabtagene ciloleucel or tisagenlecleucel.[12 14] In contrast, among the two relapsed patients with available biopsies in our study, both remained positive for CD19 and CD20. Although limited by the small number of biopsied cases, this finding is consistent with previous reports of bispecific CD19/20 CAR-T therapy, in which 11 of 12 relapses remained antigen positive.[21] Collectively, these observations suggest that relapse after bispecific CAR-T therapy may not be explained by antigen loss alone. Prior studies have shown that detectable CAR-T cells do not necessarily imply preserved functional activity, and antigen-positive relapse may reflect CAR-T dysfunction/exhaustion, insufficient functional persistence, or microenvironmental suppression.[14 31] Together, these findings support the possibility that resistance after bispecific CAR-T therapy can arise through mechanisms beyond target antigen loss. This question warrants further investigation.

To further explore biological sources of response heterogeneity beyond conventional clinical variables, we integrated spatially resolved single-cell transcriptomics with clinical outcomes. We identified two predominant spatial architectures—a B-cell-dominant pattern and a fibroblast-enriched/Mono/Mϕ-enriched pattern—each associated with distinct biological features linked to CAR-T efficacy. These findings are consistent with prior reports highlighting architectural heterogeneity in B-NHL[32 33] and provide a biological framework that may help explain some of the interpatient heterogeneity in clinical response, beyond product manufacturing and treatment procedures.

In B-cell-dominant tumors, durable responses were associated with transcriptional programs indicative of enhanced intrinsic apoptotic competence in malignant B cells, including upregulation of core apoptotic effectors and suppression of anti-apoptotic signaling. These results extend resistance models centered mainly on antigen escape[12 34] or T-cell dysfunction[35] by suggesting that tumor cell-intrinsic susceptibility to apoptosis may represent an additional contributor to CAR-T efficacy. Conversely, in fibroblast-enriched and Mono/Mϕ-enriched tumors, response appeared to be more closely associated with microenvironmental immunologic accessibility. Long-term responders exhibited a chemokine-rich niche, predominantly driven by Mono/Mϕ populations, that spatially colocalized with T cell-recruiting signals. This organization may facilitate CAR-T cell recruitment and engagement and is consistent with broader immuno-oncology literature implicating chemokine-mediated T-cell trafficking in effective antitumor immunity.[36–38]

Together, our findings support a conceptual model in which CAR-T responsiveness in B-NHL may be influenced by two partially architecture-associated axes: tumor-intrinsic apoptotic vulnerability and microenvironment-mediated immunological accessibility. If validated in larger cohorts, pretreatment spatial biopsy profiling may help refine patient stratification and guide rational combination strategies. For example, tumors with relative apoptotic resistance may be rational candidates for apoptosis-sensitizing approaches, such as BH3 mimetic-based strategies,[39 40] whereas stromal-enriched/myeloid-enriched or immune-excluded tumors may be better suited for approaches aimed at remodeling suppressive microenvironmental barriers or enhancing chemokine-guided CAR-T trafficking and engagement.[13 41 42] These observations support the potential clinical utility of spatial architectural and transcriptomic features not only as predictive biomarkers, but also as a basis for biomarker-guided therapeutic intensification.

Our study has several limitations. The spatial transcriptomic cohort was modest in size, and causal mechanisms

require validation in larger cohorts and functional models. Spatial profiling offers only a static view and cannot fully capture dynamic CAR-T trafficking or tumor-immune interactions. Moreover, although the transcriptional signatures implicate apoptotic and chemotactic pathways, their functional relevance remains to be defined through perturbational studies and prospective clinical evaluation. Despite these limitations, our findings highlight previously underappreciated tumor-intrinsic and microenvironmental features associated with CAR-T efficacy in B-NHL and underscore the utility of spatially resolved analyses in elucidating therapeutic response. Larger, integrated studies will be required to determine whether spatial architecture can serve as a clinically actionable biomarker.

CONCLUSIONS

In summary, this study demonstrates the safety and durable clinical activity of bispecific CD19/20 CAR-T therapy in heavily pretreated patients with relapsed or refractory B-cell NHL, underscoring the therapeutic potential of dual-antigen targeting. Our findings further suggest that CAR-T responsiveness may be associated with either tumor-intrinsic apoptotic vulnerability or microenvironment-mediated immunologic accessibility, with these factors predominating in distinct spatial tumor architectures. If validated, pretreatment spatial biopsy profiling may help refine patient stratification and guide biomarker-informed combination strategies.

Author affiliations
[1]Department of Hematology and Oncology, Shenzhen University General Hospital, International Cancer Center, Hematology Institution, Haoshi Cell Therapy Institute of Shenzhen University, Shenzhen University Medical School, Shenzhen University, Shenzhen, China
[2]Department of Pathology, Shenzhen University General Hospital, Shenzhen University, Shenzhen, China
[3]Shenzhen Haoshi Biotechnology Co., Ltd, Shenzhen, China

Acknowledgements We thank Hanhui Hong (Accuramed Biotech Co., Ltd., Guangzhou, China) for technical assistance with 10x Genomics Visium HD spatial transcriptomic data analysis.

Contributors Conceptualization of the project: LixinW, CF, YL, and LY. Development of methodology: LixinW, CF, YL, and LY. Collection, analysis, and interpretation of data: CF, YZ, YX, WH, WZ, YW, JX, KT, LeiW, HP, XG, SW, LijunW, LL, JQ, XM, ZH, ZW, CY, JM, HW, and YL. Writing articles and revision of the manuscript: LixinW, CF, YL, and LY. All authors approved the final manuscript as submitted and agree to be accountable for all aspects of the work. LixinW and CF contributed equally. LY is the guarantor of the study.

Funding Shenzhen Medical Research Fund (C2301003), National Natural Science Foundation of China (82470229, 82030076), Shenzhen Clinical Research Center for hematologic disease (20230731103645009), Shenzhen Science and Technology Program (JCYJ20241202124225031), Program for Youzuzhikeyan of Shenzhen University, Sanming Project of Medicine in Shenzhen (SZSM202111004), Shenzhen Key Laboratory Foundation (ZDSYS20200811143757022), Medicine Plus Program of Shenzhen University (000003011601), HaiYa Young Scientist Foundation of Shenzhen University General Hospital (HY002), Shenzhen Natural Science Fund (the Stable Support Plan Program, 20200830182623001). The funders had no role in study design, data collection, data analysis, data interpretation, writing of the report, or the decision to submit the article for publication.

Competing interests No, there are no competing interests.

Patient consent for publication Not applicable.

Ethics approval This study was approved by the ethics committee of Shenzhen University General Hospital (SUGHKYLL202205010-3) and was registered with ClinicalTrials.gov (NCT04723914). Informed consent was obtained from all enrolled patients.

Provenance and peer review Not commissioned; externally peer reviewed.

Data availability statement Data are available upon reasonable request. The datasets generated during and/or analyzed during the current study are available from the corresponding author on reasonable request.

ORCID iD
Chuling Fang https://orcid.org/0000-0002-8381-1823

REFERENCES

1 Elstrom RL, Martin P, Ostrow K, *et al*. Response to second-line therapy defines the potential for cure in patients with recurrent diffuse large B-cell lymphoma: implications for the development of novel therapeutic strategies. *Clin Lymphoma Myeloma Leuk* 2010;10:192–6.
2 Crump M, Neelapu SS, Farooq U, *et al*. Outcomes in refractory diffuse large B-cell lymphoma: results from the international SCHOLAR-1 study. *Blood* 2017;130:1800–8.
3 Hamadani M, Hari PN, Zhang Y, *et al*. Early failure of frontline rituximab-containing chemo-immunotherapy in diffuse large B cell lymphoma does not predict futility of autologous hematopoietic cell transplantation. *Biol Blood Marrow Transplant* 2014;20:1729–36.
4 Neelapu SS, Jacobson CA, Ghobadi A, *et al*. Five-year follow-up of ZUMA-1 supports the curative potential of axicabtagene ciloleucel in refractory large B-cell lymphoma. *Blood* 2023;141:2307–15.
5 Abramson JS, Palomba ML, Gordon LI, *et al*. Two-year follow-up of lisocabtagene maraleucel in relapsed or refractory large B-cell lymphoma in TRANSCEND NHL 001. *Blood* 2024;143:404–16.
6 Schuster SJ, Tam CS, Borchmann P, *et al*. Long-term clinical outcomes of tisagenlecleucel in patients with relapsed or refractory aggressive B-cell lymphomas (JULIET): a multicentre, open-label, single-arm, phase 2 study. *Lancet Oncol* 2021;22:1403–15.
7 Neelapu SS, Chavez JC, Sehgal AR, *et al*. Three-year follow-up analysis of axicabtagene ciloleucel in relapsed/refractory indolent non-Hodgkin lymphoma (ZUMA-5). *Blood* 2024;143:496–506.
8 Morschhauser F, Dahiya S, Palomba ML, *et al*. Lisocabtagene maraleucel in follicular lymphoma: the phase 2 TRANSCEND FL study. *Nat Med* 2024;30:2199–207.
9 Dreyling M, Fowler NH, Dickinson M, *et al*. Durable response after tisagenlecleucel in adults with relapsed/refractory follicular lymphoma: ELARA trial update. *Blood* 2024;143:1713–25.
10 Wang M, Siddiqi T, Gordon LI, *et al*. Lisocabtagene Maraleucel in Relapsed/Refractory Mantle Cell Lymphoma: Primary Analysis of the Mantle Cell Lymphoma Cohort From TRANSCEND NHL 001, a Phase I Multicenter Seamless Design Study. *J Clin Oncol* 2024;42:1146–57.
11 Furqan F, Shah NN. Bispecific CAR T-cells for B-cell Malignancies. *Expert Opin Biol Ther* 2022;22:1005–15.
12 Plaks V, Rossi JM, Chou J, *et al*. CD19 target evasion as a mechanism of relapse in large B-cell lymphoma treated with axicabtagene ciloleucel. *Blood* 2021;138:1081–5.
13 Locke FL, Filosto S, Chou J, *et al*. Impact of tumor microenvironment on efficacy of anti-CD19 CAR T cell therapy or chemotherapy and transplant in large B cell lymphoma. *Nat Med* 2024;30:507–18.

14 Ruella M, Korell F, Porazzi P, *et al*. Mechanisms of resistance to chimeric antigen receptor-T cells in haematological malignancies. *Nat Rev Drug Discov* 2023;22:976–95.
15 Dai H, Wu Z, Jia H, *et al*. Bispecific CAR-T cells targeting both CD19 and CD22 for therapy of adults with relapsed or refractory B cell acute lymphoblastic leukemia. *J Hematol Oncol* 2020;13:30.
16 Wang L, Fang C, Kang Q, *et al*. Bispecific CAR-T cells targeting CD19/20 in patients with relapsed or refractory B cell non-Hodgkin lymphoma: a phase I/II trial. *Blood Cancer J* 2024;14:130.
17 Cheson BD, Fisher RI, Barrington SF, *et al*. Recommendations for initial evaluation, staging, and response assessment of Hodgkin and non-Hodgkin lymphoma: the Lugano classification. *J Clin Oncol* 2014;32:3059–68.
18 Lee DW, Santomasso BD, Locke FL, *et al*. ASTCT Consensus Grading for Cytokine Release Syndrome and Neurologic Toxicity Associated with Immune Effector Cells. *Biol Blood Marrow Transplant* 2019;25:625–38.
19 Tong C, Zhang Y, Liu Y, *et al*. Optimized tandem CD19/CD20 CAR-engineered T cells in refractory/relapsed B-cell lymphoma. *Blood* 2020;136:1632–44.
20 Ying Z, Yang H, Guo Y, *et al*. Long-term outcomes of relmacabtagene autoleucel in Chinese patients with relapsed/refractory large B-cell lymphoma: Updated results of the RELIANCE study. *Cytotherapy* 2023;25:521–9.
21 Zhang Y, Wang Y, Liu Y, *et al*. Long-term activity of tandem CD19/CD20 CAR therapy in refractory/relapsed B-cell lymphoma: a single-arm, phase 1-2 trial. *Leukemia* 2022;36:189–96.
22 Zurko JC, Fenske TS, Johnson BD, *et al*. Long-term outcomes and predictors of early response, late relapse, and survival for patients treated with bispecific LV20.19 CAR T-cells. *Am J Hematol* 2022;97:1580–8.
23 Yu W, Li P, Zhou L, *et al*. A phase 1 trial of prizloncabtagene autoleucel, a CD19/CD20 CAR T-cell therapy for relapsed/refractory B-cell non-Hodgkin lymphoma. *Blood* 2025;145:1526–35.
24 Spiegel JY, Patel S, Muffly L, *et al*. CAR T cells with dual targeting of CD19 and CD22 in adult patients with recurrent or refractory B cell malignancies: a phase 1 trial. *Nat Med* 2021;27:1419–31.
25 Roddie C, Lekakis LJ, Marzolini MAV, *et al*. Dual targeting of CD19 and CD22 with bicistronic CAR-T cells in patients with relapsed/refractory large B-cell lymphoma. *Blood* 2023;141:2470–82.
26 Landsburg DJ, Frigault MJ, Heim M, *et al*. Real-world outcomes with tisagenlecleucel in aggressive B-cell lymphoma: subgroup analyses from the CIBMTR registry. *J Immunother Cancer* 2025;13:e009890.
27 Hirayama AV, Gauthier J, Hay KA, *et al*. The response to lymphodepletion impacts PFS in patients with aggressive non-Hodgkin lymphoma treated with CD19 CAR T cells. *Blood* 2019;133:1876–87.
28 Rabinovich E, Pradhan K, Sica RA, *et al*. Elevated LDH greater than 400 U/L portends poorer overall survival in diffuse large B-cell lymphoma patients treated with CD19 CAR-T cell therapy in a real world multi-ethnic cohort. *Exp Hematol Oncol* 2021;10:55.
29 Yegya-Raman N, Plastaras JP, Wright CM, *et al*. Bridging radiotherapy before chimeric antigen receptor T cells for B-cell lymphomas: an ILROG multicenter study. *Blood Adv* 2025;9:3293–303.
30 Ho PJ, Vanguru V, Burge CS, *et al*. Real-world Australian experience with tisagenlecleucel for relapsed/refractory diffuse large B-cell lymphoma-importance of pre-CAR-T optimization. *Front Oncol* 2025;15:1633644.
31 López-Cantillo G, Urueña C, Camacho BA, *et al*. CAR-T Cell Performance: How to Improve Their Persistence? *Front Immunol* 2022;13:878209.
32 Colombo AR, Hav M, Singh M, *et al*. Single-cell spatial analysis of tumor immune architecture in diffuse large B-cell lymphoma. *Blood Adv* 2022;6:4675–90.
33 Dai Y, Kizhakeyil A, Chihara D, *et al*. Multi-modal spatial characterization of tumor immune microenvironments identifies targetable inflammatory niches in diffuse large B cell lymphoma. *Nat Genet* 2025;57:2715–27.
34 Zhang Z, Chen X, Tian Y, *et al*. Point mutation in *CD19* facilitates immune escape of B cell lymphoma from CAR-T cell therapy. *J Immunother Cancer* 2020;8:e001150.
35 Wu A, Zhang T, Yu H, *et al*. Mechanisms underlying resistance to CAR-T cell therapy and strategies for enhancement. *Cytokine Growth Factor Rev* 2025;83:66–76.
36 Karin N. Chemokines and cancer: new immune checkpoints for cancer therapy. *Curr Opin Immunol* 2018;51:140–5.
37 Wu B, Zhang B, Li B, *et al*. Cold and hot tumors: from molecular mechanisms to targeted therapy. *Signal Transduct Target Ther* 2024;9:274.
38 Ozga AJ, Chow MT, Luster AD. Chemokines and the immune response to cancer. *Immunity* 2021;54:859–74.
39 Lee YG, Guruprasad P, Ghilardi G, *et al*. Modulation of BCL-2 in Both T Cells and Tumor Cells to Enhance Chimeric Antigen Receptor T-cell Immunotherapy against Cancer. *Cancer Discov* 2022;12:2372–91.
40 Yang M, Wang L, Ni M, *et al*. Pre-sensitization of Malignant B Cells Through Venetoclax Significantly Improves the Cytotoxic Efficacy of CD19.CAR-T Cells. *Front Immunol* 2020;11:608167.
41 Adachi K, Kano Y, Nagai T, *et al*. IL-7 and CCL19 expression in CAR-T cells improves immune cell infiltration and CAR-T cell survival in the tumor. *Nat Biotechnol* 2018;36:346–51.
42 Lei W, Zhao A, Liu H, *et al*. Safety and feasibility of anti-CD19 CAR T cells expressing inducible IL-7 and CCL19 in patients with relapsed or refractory large B-cell lymphoma. *Cell Discov* 2024;10:5.